Turkish Computational and Theoretical Chemistry

Turkish Comp Theo Chem (TC&TC)

Volume(Issue): 8(3) – Year: 2024 – Pages: 74-98

e-ISSN: 2602-3237

https://doi.org/10.33435/tcandtc.1386285

Received: 05.11.2023 ***Accepted:*** 04.02.2024 *Research Article*

Molecular design and virtual screening of novel heterocyclic derivatives as Glucokinase activators

Anuradha Mehra[a], Amit Mittal[a, 1], Pankaj Wadhwa[a], Aryan Mehra[b]

[a]Department of Pharmaceutical Chemistry, School of Pharmaceutical Sciences, Lovely Professional University, Jalandhar-Delhi G.T. Road (NH-1), Phagwara (Punjab) 144411, India

[b]Department of Mechanical Engineering, Lovely Professional University, Jalandhar-Delhi G.T. Road (NH-1), Phagwara (Punjab) 144411, India

Abstract: Deficiency of insulin signaling in type 2 diabetes results from insulin resistance or defective insulin secretion and induce hyperglycemia. Diabetes is a global threat that continues to increase day by day at a very high rate in both developing and developed countries. Glucokinase activators (GKA) can be a novel target used for better management of type 2 diabetes. Recently novel GKA Dorzagliatin received market approval by Japan FDA for treatment of type 2 diabetes. The purpose of designing glucokinase activators was to develop novel therapeutic molecules with minimum side effects. A docking study was conducted using AutoDock Vina 1.5.6, and the structures were created using ChemBiodraw Ultra. The Swiss ADME algorithm was used for online log p prediction. Among all the molecules designed, AM35 had the highest binding affinity to GK receptors. For good absorption and elimination, Log P values range from 2-3.08, indicating good lipophilic properties. The new lead molecules were designed as glucokinase activators, which had a better pharmacokinetic profile and higher binding affinity.

Keywords: Type 2 diabetes, Glucokinase activator, molecular docking, AutoDock Vina.

1. Introduction

Type 2 Diabetes Mellitus is marked by several distinctive features, which encompass heightened production of glucose in the liver, reduced sensitivity to insulin, compromised insulin release, and irregular fat processing [1]. During the initial phases of the condition, the pancreas' beta cells augment their insulin release as a response to the emerging insulin resistance, thereby maintaining relatively normal glucose tolerance [2, 3]. Nevertheless, in some individuals, the pancreatic islets eventually struggle to sustain this state of heightened insulin production and resistance as compensatory mechanisms wane. This progression results in impaired glucose tolerance, evident through elevated post-meal glucose levels [4, 5]. As the disease advances, overt diabetes becomes apparent, characterized by elevated fasting blood sugar due to decreased insulin secretion and heightened hepatic glucose synthesis [6, 7]. The escalating global menace of diabetes continues to surge, with its prevalence steadily increasing across the world, spanning both developed and developing nations [8]. According to the Tenth Edition of the IDF Diabetes Atlas 2021, a staggering 537 million adults aged 20 to 79 are grappling with diabetes, with the year 2021 witnessing a distressing 6.7 million diabetes-related fatalities [9, 10]. Projections indicate that the number of individuals affected by diabetes will soar to 643 million by 2030 and an even higher 783 million by 2045 [11, 12]. A significant majority, about 81%, of adults afflicted by diabetes are situated in low and middle-income economies. Over the last 15 years, diabetes has accounted for at least USD 966 billion (a 316% increase) in healthcare expenditures [13, 14]. Of utmost concern is the fact that nearly half, specifically 46.5%, of adults with diabetes remain undiagnosed. Glucokinase (GK) is an enzyme located in the cytoplasm that facilitates the

[1] Corresponding Authors

e-mail: amitmittal77@yahoo.com, amit.31641@lpu.co.in

conversion of glucose into glucose-6-phosphate through phosphorylation [15]. The primary sites of GK expression are the pancreatic β-cells and hepatocytes within the liver. In the β-cells of the pancreas, GK serves as a molecular detector, triggering insulin release in response to glucose stimulation [16, 17]. The extent of glucose phosphorylation in pancreatic β-cells is directly proportional to the glucose concentration, regulating the rate of insulin secretion [18]. By regulating both glycolysis and ATP production, glucokinase preserves optimal ATP/ADP ratios. When the membrane potential reaches a specific threshold, GK prompts the opening of L-type calcium channels. This Ca2+-dependent process leads to insulin release. Activation of GK contributes to the restoration of insulin secretion and calcium response in pancreatic islets. In hepatocytes, GK plays a pivotal role in glucose metabolism [19]. Its activity is modulated by glucokinase regulatory protein (GKRP), an inherent inhibitor. At low glucose levels, GK is inactive and bound to GKRP in the nucleus. GK activators (GKAs) bind to an allosteric site on the enzyme. They can activate GK directly and disrupt the GK/GKRP complex, causing its dissociation. As blood glucose levels rise, GK translocates to the cytoplasm [20]. GKAs not only enhance insulin secretion but also foster glycolysis and glycogen synthesis, thereby improving glucose tolerance. In 2003, Hoffmann-La Roche AG introduced the GKA compound RO-281675, which amplified GK's maximum metabolic rate (Vmax) by 1.5-fold at 3 μM concentration. The glucose concentration (S0.5) required for half of Vmax decreased from 86 mM to 20 mmol/L [21]. Despite its potential as a diabetes management tool, this compound never underwent clinical trials due to cardiovascular risks. However, its development inspired other pharmaceutical companies to create efficient and safe GKAs [22]. In recent years, a range of molecules with heterocyclic structures—containing nitrogen, sulfur, oxygen, and amide linkages—have emerged as potential GK activators in Figure 1. These molecules interact with GK's allosteric site, prompting researchers to explore alternative core nuclei for developing novel GKAs with superior potency, efficacy, enhanced physicochemical properties, and reduced toxicity [23]. Research has been driven to find potent glucokinase activators with fewer adverse effects due to current drugs' ineffectiveness and side effects. Computer simulations, software is used to assemble, prepare, process, and evaluate data as well as construct and evaluate models. In addition to being economical, computer-aided designs make experiments and predictions easier to assess [24]. Therefore, our current research work focused on building a virtual library of heterocyclic derivatives, investigating their binding affinity to GK active pockets, and analyzed their pharmacokinetics and toxicity profiles [25].

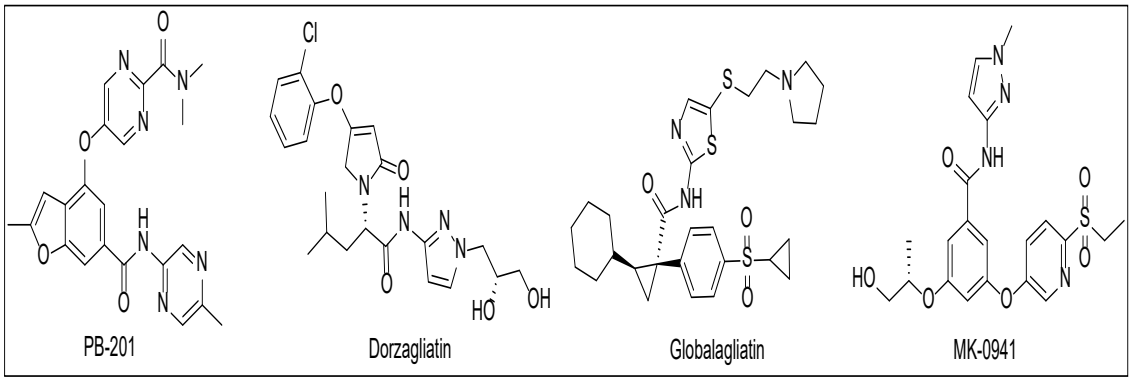

Figure 1. Glucokinase activators available in Market.

Montano et al. designed benzimidazole derivatives as GKAs and study revealed compound 1, in Figure 2, showed good potential as a blood glucose control drug since presenting an increase of GK (2.86 and 3.74-fold at 100 and 200 μg mL−1) (26). Sharma & co-workers synthesized pyridine amide derivatives and analysed their GK activation potential. Based on their docking scores compound 2, in Figure 2, demonstrate highest binding affinity of -9.1 kcal/mol (27). Hamid et al. designed benzene sulphonamide derivatives and in vitro enzymatic activity assay results compound 3, in Figure 2,

exhibits 1.37 fold GK activation (28). Kazi & colleagues performed in-silico designing of benzamide derivatives as GKAs. Docking studies revealed 4 (Figure 2) binding interactions with Arg 63 residue for the best-fit conformations in the binding site of the GK enzyme and show 1.5 fold GK activation (29). Arora et al. designed N-benzothiazol-2-yl is attached to the benzamide nucleus to form novel derivatives as GKA. Compound 5 (Figure 2) exhibit effective GK activation by 1.97 folds (30). Khadse & co-workers synthesized sulfonamido-benzamide hybrids and compound 6 show EC50 as 495 nM. In-vivo OGTT assay, compound 6 (Figure 2) disclosed an extreme decrease in blood glucose level as 135 mg/dL (31). In another study conducted by Khadse & group include design, synthesis, and evaluation of quinazolin-4-one derivatives as GKAs. Compound 7 (Figure 2) with EC50 of 516 nM demonstrate the highest in vitro GK activation (32). Grewal et al. synthesized 3,5-disubstituted benzamide derivatives as GKA. Compound 8 (Figure 2) exhibit promising GK activity as 2.11 µM and 250 mg/dL glucose reduction at 120 min interval in OGTT assay (33). Charaya & colleagues aimed to enhance the activity of GK in the benzamide nucleus, thiazol-2yl is substituted at amido nitrogen and aromatic moieties are substituted at the sulfonamide group. In vivo OGTT assay results demonstrate compound 9 (Figure 2) reduces blood glucose equipotent to that of the standard drug (metformin blood glucose level reduction is 125 mg/dL) at 120 min time interval (34). Kohn et al. designed and evaluate the GK activity of the prepared 5-alkyl-2-urea-substituted pyridines derivatives. A dose-proportional diminution in blood glucose levels was observed when compound 10 (Figure 2) was administered at doses of 3, 10, 30, and 100 mg/kg during OGTT assay, displaying a 40% reduction in AUC at 100 mg/kg (35).

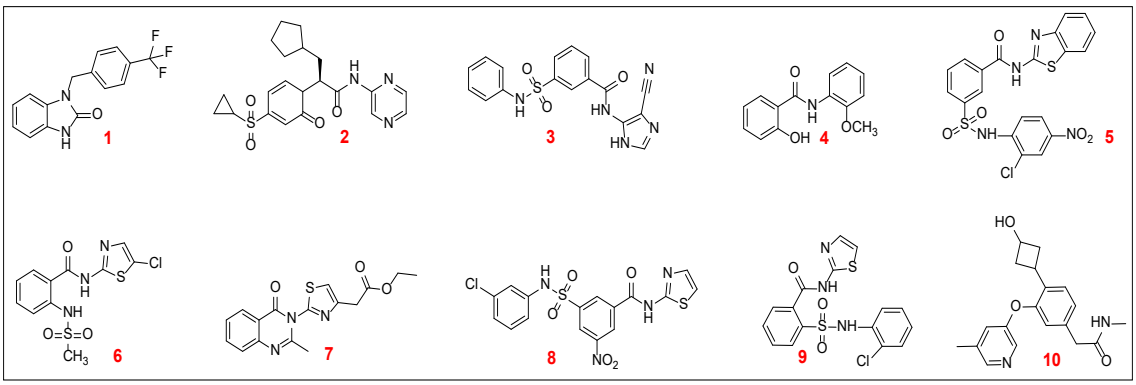

Figure 2. Glucokinase activators (compounds 1-10) explored in the literature review

Glucokinase, a member of the hexokinase enzyme family, undergoes activation upon stimulation. Activating the GK enzyme is triggered by GKA interacting with its allosteric site (36). Functioning as a discerning "glucose sensor," GK orchestrates insulin secretion in the pancreatic β-cells, responding dynamically to glucose levels (37). The liver's glycogen synthesis and storage are promoted by GK, a key glucose "gatekeeper." GK activation by small molecules has been proposed as an innovative method to enhance glycemic control in patients with diabetes (38, 39). GK functions as a molecular sentinel within pancreatic beta cells for insulin release in response to glucose stimulation (40). A novel heterocyclic derivative of GKA propels the activity of GK by firmly binding to it. GK catalyzes glucose phosphorylation within pancreatic acinar cells, a process directly related to glucose concentration. So, regulation of insulin secretion is determined by glucose phosphorylation rate (41). ADP/ATP ratios are maintained by glucokinase's modulation of glycolysis and oxidative ATP production. Insulin is released calcium-dependently when GK reaches its membrane potential threshold. As a result of this process, GK activation restores insulin secretion in pancreatic islets (Figure 3) and calcium response to glucose (42). This intricate pathway enables novel heterocyclic derivatives to produce hypoglycemic agents capable of reducing blood glucose levels, an important component of the management of type 2 diabetes (43).

Among antidiabetic drugs, metformin is associated with drug resistance when used in long-term use.

Furthermore, conventional oral hypoglycaemic drugs (e.g. pyrazolidines, sulfonylureas and acarbose) may cause severe side effects and have sundry drawbacks (e.g. poor efficacy). Thus, it is imperative to develop new anti-diabetic drugs. By increasing glucose uptake and lowering blood glucose levels, glucokinase activators exhibit promising treatment of type 2 diabetes. In spite of this, it is important to design GKAs that are effective as well as minimally side effects. The liver and pancreas should be the only organs targeted by GKAs without adversely affecting other organs such as the brain or the heart. It is expected that GKAs will not adversely affect other physiological processes, such as insulin sensitivity and lipid metabolism. Studies examining chronic GKA use need to be conducted for an accurate assessment of potential risks. Resistance to oral antidiabetic drugs should be overcome by GKAs.

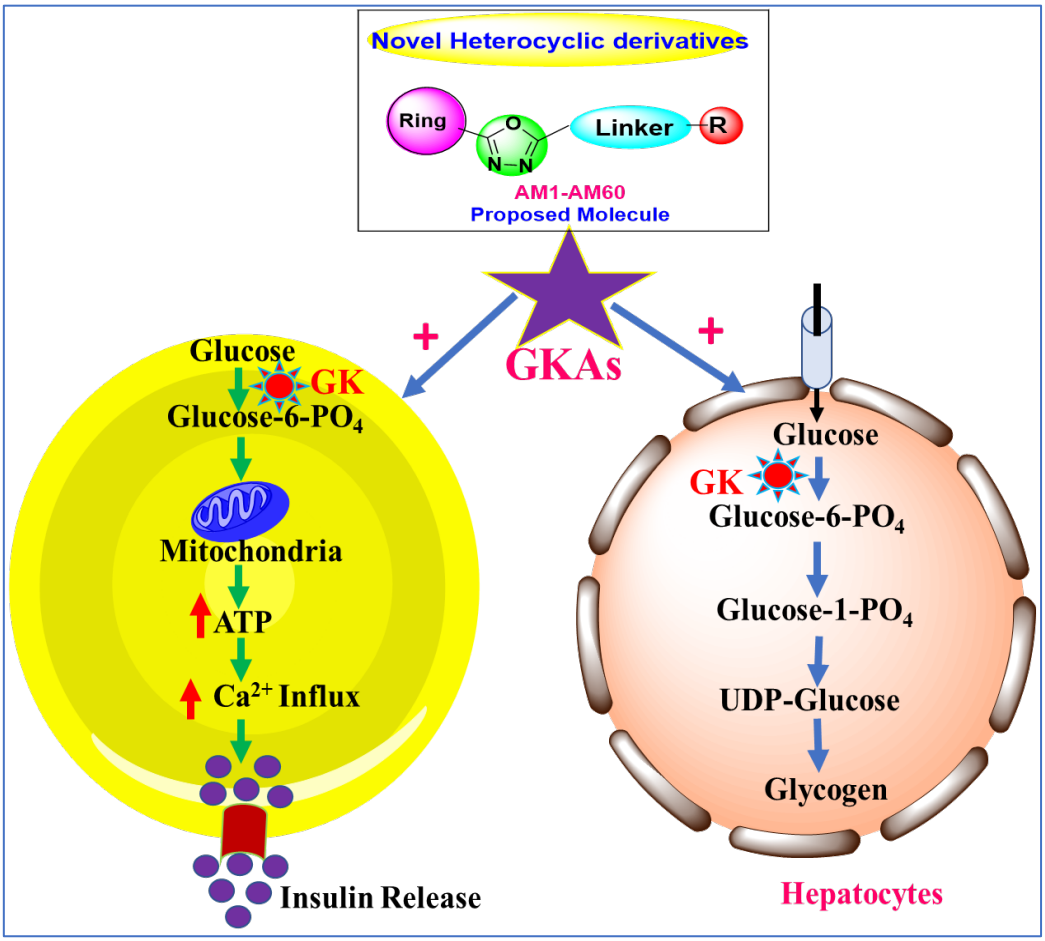

Figure 3. Mechanism of action of novel heterocyclic derivatives as GKAs

Development of strategies for preventing or reversing drug resistance requires an understanding of the molecular mechanisms underlying resistance. It may be possible to improve glucose control in T2DM patients by combining GKAs with other antidiabetic drugs, such as metformin. In light of this, combination therapies targeting different aspects of glucose metabolism could provide a promising approach for T2DM. The current landscape of GKA drugs has significant research gaps and challenges, particularly regarding their safety and efficacy over the long term. A comprehensive understanding of their extended safety profiles remains elusive, despite their potential to improve glycemic control through glucokinase activation. Several challenges stand in the way of more effective development of GKAs, including the variability of each patient's response, the possibility of off-target effects, and the limited knowledge available about the intricate mechanisms influenced by these proteins. It is also difficult to implement these interventions in practice because of issues such as patient adherence, variability in pharmacokinetics, and the

need for effective patient stratification. Development of novel heterocyclic derivatives has the potential to advance GKA therapies in the future. In addition to providing greater specificity, efficacy, and safety, these derivatives could help address today's challenges. Through this research, new insights could be gained into glucokinase activation, mechanistic insights could be uncovered, and new therapeutic strategies could be developed to effectively manage diabetes. In order to advance the field and ultimately improve treatment outcomes for diabetic patients, comprehensive investigations into their pharmacological properties, safety profiles, and potential synergies are imperative.

2. Computational Method

2.1. Research tools

Vina 1.5.6 AutoDock (44) tool is used to analyze GK activation in terms of binding affinity (Kcal/mol) and compare them with the molecules' best-docked conformation binding affinity score. 2D and 3D structure of the compounds was created using ChemBiodraw ultra and ChemBiodraw 3D software. By employing the MM2 approach, each molecule's energy was minimised so that its performance could be maximized. Also, AutoDock Vina transformed the derivatives' format into a more decipherable format. Glucokinase activation was identified by downloading proteins with the PDB ID 1V4S from the protein data bank (45). Examining the results of compound interactions involved utilizing Biovia Discovery Studio Visualizer (46) and Pymol software (47) to ascertain their poses.

2.2. Default Directory Setup

In Autodock, the default directory setup was done using following steps: Go to File > Preferences > Set, input C:\workspace under Startup directory, click Set, and then Make default. This process establishes the default directory as the default storage location for all docking files.

2.3. Protein Selection and Preparation

The glucokinase activation activity was determined using the pdb code 1V4S from the RCSB Protein Data Bank (https://www.rcsb.org/). The protein was then loaded into the AutoDock Vina software program for extraction of the protein and ligand individually. The main goal of this software is to find potential hit compounds with high binding affinity.

The desktop shortcut provided access to the AutoDock tool. Open the macromolecule file (1V4S.pdb) in the workspace folder by selecting File > Read Molecule. The water can be removed by selecting Edit > Delete Water. The macromolecule can be hydrogenated by clicking Edit > Hydrogens > Add > All Hydrogens > OK. Non-polar hydrogen can be merged with other non-polar hydrogen by selecting Edit > Hydrogen > Merge Non-Polar. Using the Edit > Charges menu, click Compute Gasteiger and add all the Gasteiger charges that were calculated. Modifications can be saved by selecting File > Save > Write PDB > OK. Workspace folder is updated with the updated pdb file when this action is performed. Select the macromolecule under Grid > Macromolecules > Choose > OK. It should be saved as "protein.pdbqt" in the same folder where the pdb files are kept.

2.4. Validation of Protein for Docking

An analysis of the ligand structure has been conducted using a protein structure (.pdb) file, 1V4S, which is docked repeatedly with the binding site. A RMSD (Root Mean Square Deviation) analysis was conducted in order to determine reproducibility and validity of the method based on redocked binding sites with ligand atoms and crystallographic conformations.

2.5. Ligand Preparation

An extensive library of heterocyclic derivatives was screened in order to determine which one had the best binding affinity. ChemBioDraw 2D was then used to create the 2D structures. Additionally, three-dimensional structures of the ligands were created with ChemBioDraw 3D. Autodock Vina software1.5.6 program to analyze the ligands, the ligands were stored as .pbd files.

Open the ligand file "AM1.pdb" within AutoDock by selecting Ligand > Input > Open. An AutoDock analyzes the structure of a ligand, incorporating charges and identifying rotational bonds autonomously. In this instance, a noteworthy discovery unfolded, revealing number of aromatic carbons and the detection of number of rotatable bonds. To detect the root, proceed with select Ligand > Torsion Tree > Detect root. Within the

AutoDock visualization window, a green circle will indicate the presence of the root. The ligand file can be saved by choosing Ligand > Output > Save as pdbqt. Each subsequent ligand from AM2 to AM60 should be meticulously replicated in this manner.

2.6. Configuring Grid Spacing

Identifying potential binding sites for a macromolecule based on grid box boundaries. Choosing 1V4S.pdb by Navigating to Grid > Macromolecule > Choose. In the same workspace, save the updated Macromolecule as a pdbqt file. Choose ligand > Select MRK > Click ligand in Grid > Set map types. The Grid Box can be accessed by selecting Grid > Grid Box. The current setup will be saved after selecting File > Close. The next step is to navigate to Grid > Output > Save. Save the file in the workspace folder with the name "conf".

2.7. Molecular Docking Study

To find the hit GK activators, a molecular modelling tool was used to examine the designed library of molecules. Based on the binding of GK active site, the selected 1V4S protein was engendered. By removing its ligand, the protein was validated, then polar hydrogen bonds were added, root was identified, and the file was transformed into the (.pdbqt) format. Further, to produce the 1V4S protein, water molecules were eliminated, any missing atoms were replaced, only polar hydrogen was added, and lastly, Kollman charges were included. By keeping ligand as a center, the grid box was generated. Using the grid output file, the following parameters (x, y and z dimensions) were added to the "conf.txt" configuration file.

Center_x = 40.144
Center_y = 14.796
Center_z = 62.039
Size_x = 30
Size_y = 44
Size_z = 24

A command prompt was opened and the command "program files/the Scripps research institute/vina/vina.exe - config conf.txt - log log.txt" was typed for performing molecular docking with Vina using the AutoDock Tool.

2.8. Docking Analysis

In the workspace generated following Autodock completion, select Analyze > Dockings > Open, and locate the dock.outpout file there. Select AM1.pdbqt under Analyze > Macromolecule > Choose. Additionally, select Analyze > Conformations > Play, with energy order. Following that, each conformation should be analyzed and inspected separately. Each compound should be assessed meticulously by repeating this process. Binding affinity (Kcal/mol) or docking scores were generated as output files. Based on Discovery Studio Visualizer software, *in-silico* bond length and hydrogen bond interaction were investigated for the best-designed molecules that fit the GK active pocket is summarised in table 1 below.

2.9. ADME Analysis to find the Lead Molecules

Screening and estimation of the 8 hit compounds were performed using SwissADME (http://www.swissadme.ch). Chemical structures will be imported or drew using SwissADME's molecular sketcher built on Chemaxon's Marv (48), which allows import or drawing of 2D chemical structures. Molecular SMILES can be edited, typed, or pasted since the Smile ID of each molecule is also accepted. In BIOLED-eggs, various physiochemical characteristics are observed, such as p-glycoprotein interactions, Lipinski rule of 5 (49) or drug penetration in the blood-brain barrier and gastrointestinal absorption. This computational method was used to select lead molecules with lead-like characteristics for focused GK activation.

2.10. Toxicity Prediction

pkCSM software (50) was used for the comprehensive toxicity assessment of the potent compounds AM35 and AM2. A number of parameters, including cardiotoxicity, hepatotoxicity, and others, were taken into account when predicting the results.

3. Results and discussion

3.1. Rationale Drug Design

A strategic approach to designing novel heterocyclic derivatives **AM1-AM20** for type 2 diabetes treatment relies on integrating multiple pharmacophores that are clinically proven to be anti-diabetic. Inspired by CN102558167 (GKA

filed by Institute of Materia Medica), which has demonstrated compound **A** (Figure 4) with 2.9 folds of GK activation at 10 µM, efficacious in improving insulin sensitivity, which incorporates thiazolidinedione moiety as key elements, this scaffold is incorporated in the design (51).

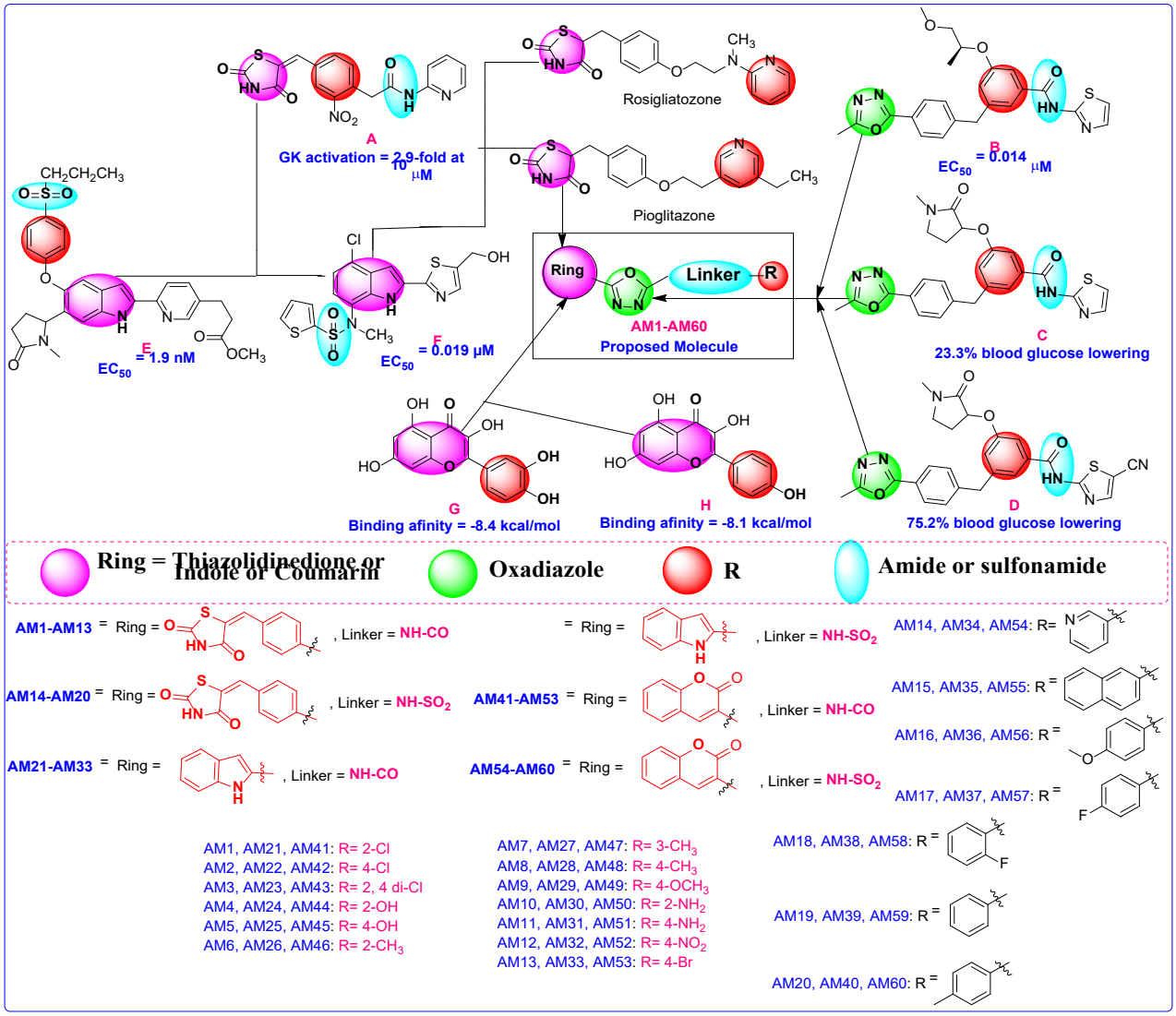

Figure 4. Rationale drug design of novel heterocyclic derivatives.

Further, as compound **B**, **C** and **D** (Figure 4) exhibit potent GK activation with EC_{50} value of 0.014 µM (*in-vitro* assay), 23.3% and 75.2% blood glucose lowering in OGTT assay respectively as disclosed in patents WO2010150280 and WO2011013141, the inclusion of an oxadiazole core enriches molecular diversity, aligning with the therapeutic benefits associated with such structures (52, 53). Compounds **A-F** (Figure 4), characterized by a common pharmacophoric feature involving amide or sulfonamide groups, have demonstrated robust activation of glucokinase, which is vital for promoting GK activity. As the design incorporates these insights, it is aimed at creating a synergistic pharmacological profile, leveraging thiazolidinedione, oxadiazole, and amide or sulfonamide functionalities in combination. As a result of systematic exploration of SAR based on the incorporation of these pharmacophores, the aim is to discover novel heterocyclic derivatives (**AM1-AM20**) with improved glucokinase activation, which may help facilitate the development of innovative and more efficacious treatments for type 2 diabetes. In light of the patent applications, US8957070B2 and WO2014099578A1 feature compounds **E** and **F** (Figure 4), considered as

robust glucokinase activators with EC_{50} value of 1.9 nM and 0.019 µM, both of which belong to the indole class (54, 55). The strategic departure in the design of heterocyclic derivatives **AM21-AM40** include replacement of thiazolidinedione ring with an indole moiety that is intended to introduce structural diversity and enhance anti-diabetic activity. In this modification, a new structural element is introduced, which may allow modulation of the molecular interaction, thus optimizing the drug's effectiveness. Grewal et al. designed natural coumarin derivatives, and through *in-silico* assessment, compound **G** and **H** (depicted in Figure 4) demonstrated significant potential as an effective treatment for type 2 diabetes by activating glucokinase with binding affinity of -8.4 and -8.1 kcal/mol (56). The effect of substituting the indole ring with the coumarin (chromene) nucleus on GK activation was explored using a comprehensive substitution strategy following the conceptualization of the proposed heterocyclic derivatives (**AM41-AM60**).

3.2. Molecular Docking

A screening was conducted using the estimated free binding energies expressed in Kcal/mol for the actively targeted GK, a glucose-sensing, which stimulates insulin secretion in pancreatic cells, and also a glucose "gatekeeper" in hepatocytes, which promotes glucose uptake as well as glycogen synthesis and storage. Compounds docked to GK proved to have higher binding affinity than the primary ligands. In the GK active pocket, MRK had a free binding energy of -7.2 Kcal/mol. An estimated binding energies of Dorzagliatin (approved by Japan FDA as GKA), Canagliflozin and Dapagliflozin (marketed antidiabetic agents) was found to be -7.2, -9.4 and -7.3 respectively. A strong binding affinity was observed for the molecules AM35, AM2, AM12, AM17, AM58, AM5, AM14, AM16, AM19, AM52 and AM57 (-11.6, -11.3, -11.1, -11.1, -11.0, -11.0, -10.8, -10.8, -10.8, -10.8, -10.8 kcal/mol respectively) when compared with MRK (-7.2 kcal/mol), Dorzagliatin (-7.2 kcal/mol), Canagliflozin (-9.4 kcal/mol), Dapagliflozin (-7.3 kcal/mol). Tables 2 and 3 list the compounds docked in the binding pockets of the target with scores and amino acids interactions that reveal binding affinities. Binding affinity of the docked molecules is between -11.6 and -10.8 Kcal/mol.

As shown in Figure 5, the MRK had hydrogen bond interactions with TYR215 and THR65. The Pi-Alkyl interactions were found with ILE211, PRO66, VAL455, VAL62, ALA456 and ILE159. The Pi-sulfur interactions with MET235 and ARg63. The Van der Waals interaction with LEU451, SER64, GLU221, TYR214, MET210 and TYR61.

Table 1. Structures and binding affinity of derivatives derived from rational drug design.

Sr. No	Compound	Structure	Binding affinity (Kcal/mol)
1.	AM1	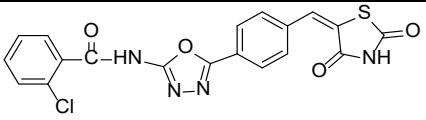	-10.0
2.	AM2	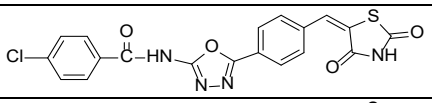	-11.3
3.	AM3	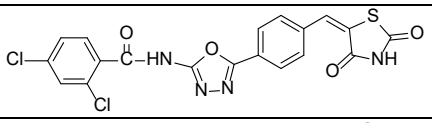	-7.7
4.	AM4	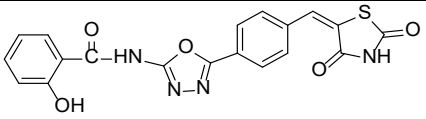	-9.1
5.	AM5	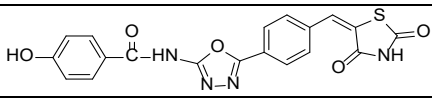	-11.0

6.	AM6	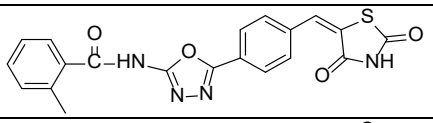	-9.0
7.	AM7	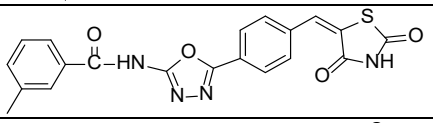	-9.9
8.	AM8	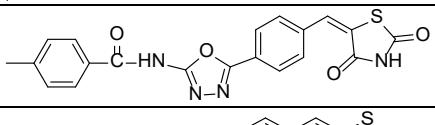	-9.7
9.	AM9	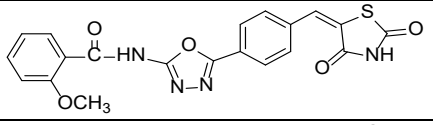	-8.2
10.	AM10	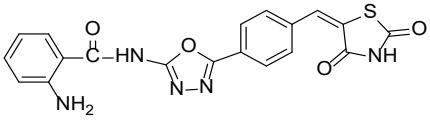	-9.1
11.	AM11	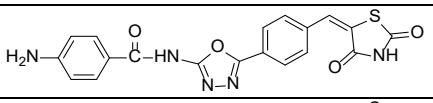	-9.5
12.	AM12	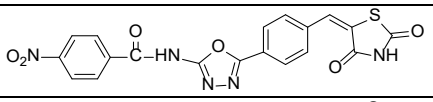	-11.1
13.	AM13	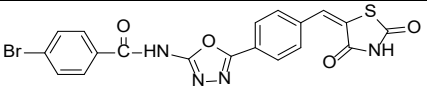	-9.7
14.	AM14	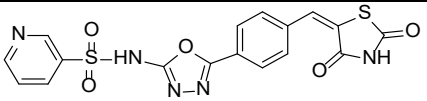	-10.8
15.	AM15	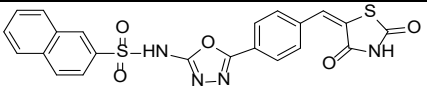	-12.4
16.	AM16	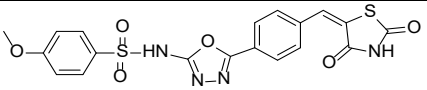	-10.8
17.	AM17	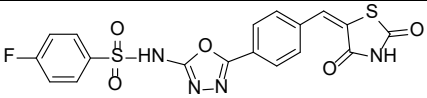	-11.1
18.	AM18	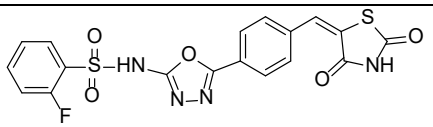	-10.7
19.	AM19	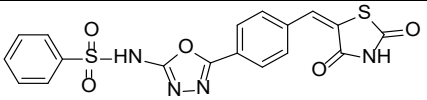	-10.8
20.	AM20	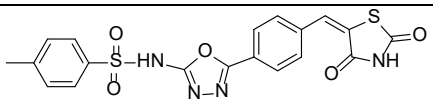	-9.8
21.	AM21	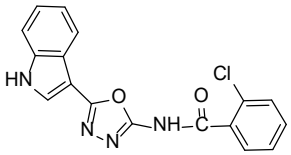	-8.8

22.	AM22	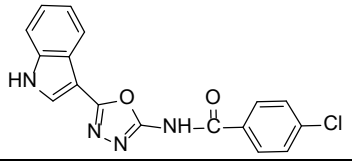	-10.1
23.	AM23	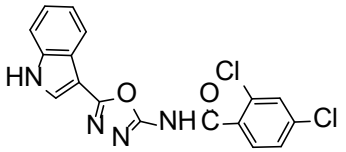	-10.4
24.	AM24	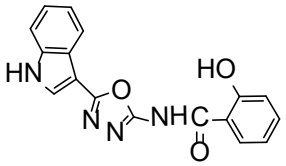	-10.6
25.	AM25	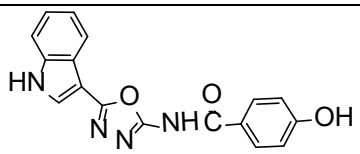	-9.7
26.	AM26	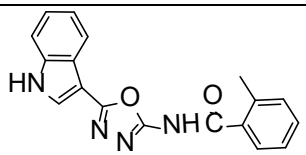	-10.5
27.	AM27	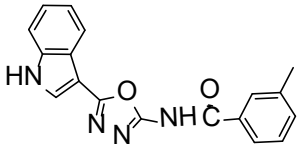	-9.9
28.	AM28	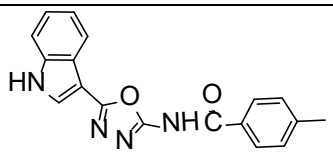	-10.4
29.	AM29	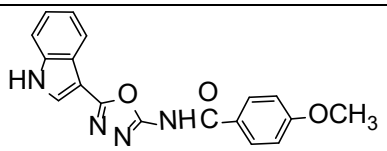	-9.9
30.	AM30	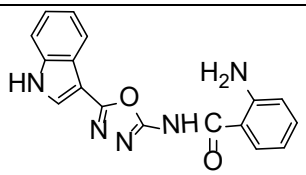	-9.7
31.	AM31	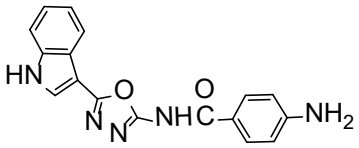	-9.9
32.	AM32	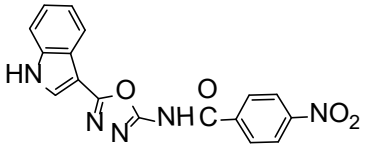	-7.6

33.	AM33	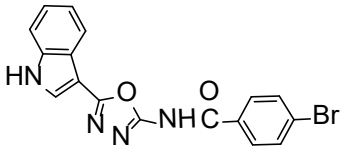	-10.3
34.	AM34	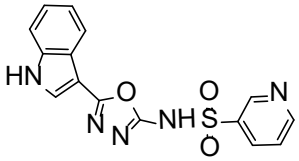	-9.7
35.	AM35	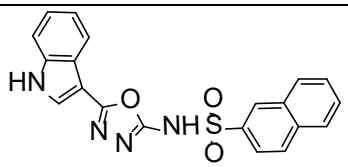	-11.6
36.	AM36	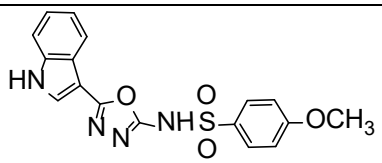	-8.8
37.	AM37	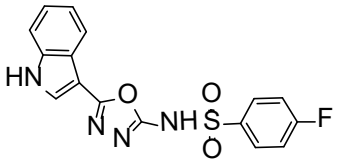	-10.2
38.	AM38	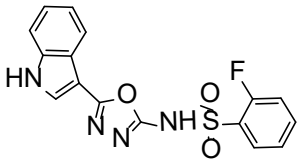	-9.8
39.	AM 39	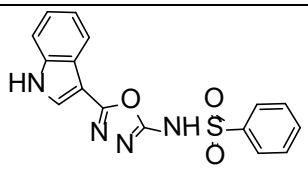	-10.1
40.	AM40	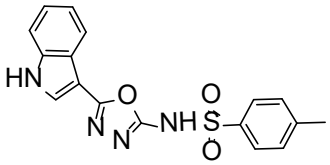	-10.7
41.	AM41	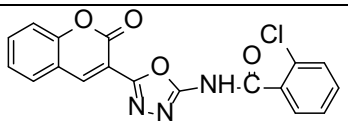	-10.2
42.	AM42	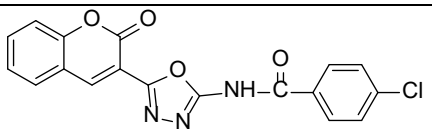	-7.8
43.	AM43	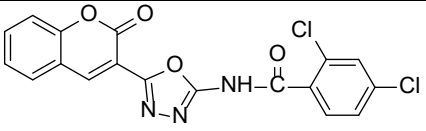	-10.4

44.	AM44	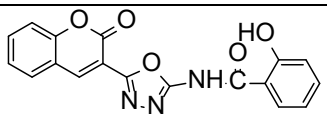	-9.7
45.	AM45	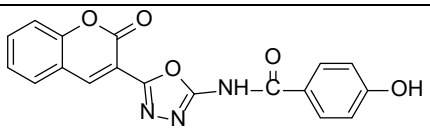	-9.6
46.	AM46	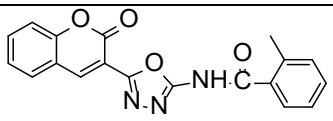	-8.6
47.	AM47	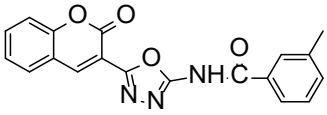	-10.1
48.	AM48	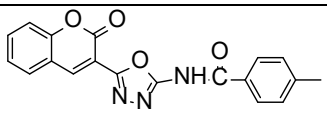	-10.6
49.	AM49	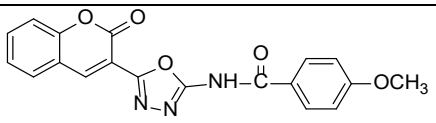	-9.6
50.	AM50	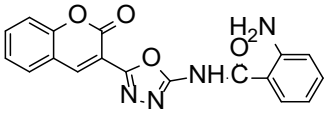	-9.7
51.	AM51	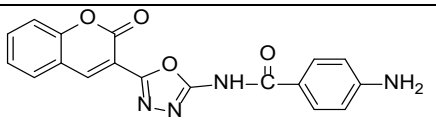	-9.9
52.	AM52	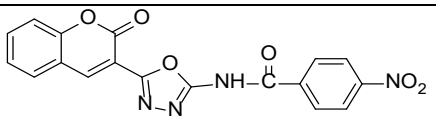	-10.8
53.	AM53	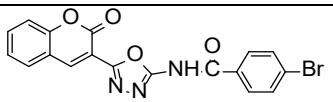	-9.8
54.	AM54	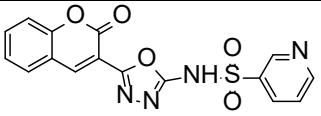	-9.8
55.	AM55	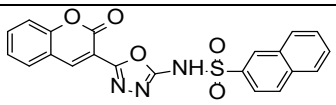	-9.8
56.	AM56	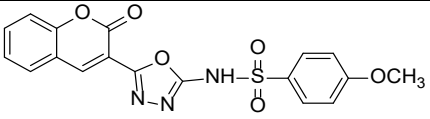	-10.6
57.	AM57	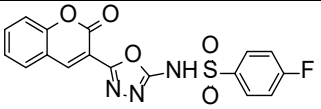	-10.8
58.	AM58	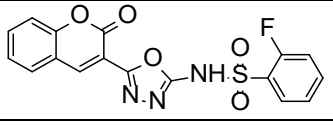	-11.0

59.	AM59	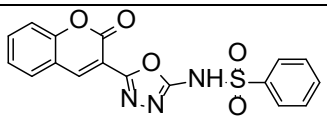	-10.6
60.	AM60	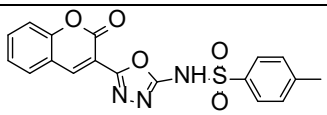	-10.4
61.	Co-cryst Ligand (MRK)	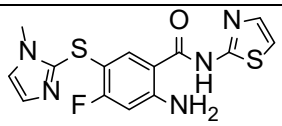	-7.2
62.	Canagliflozin	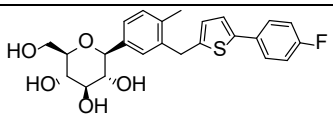	-9.4
63.	Dapagliflozin	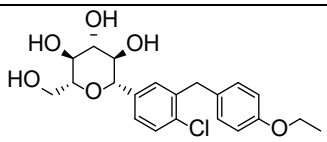	-7.3
64.	Dorzagliatin	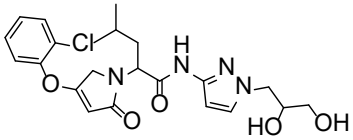	-7.2

As shown in Figure 6, the AM35 had hydrogen bond interactions with ARG63, CYS220 and THR65. The Pi-Alkyl interactions were found with ILE159, ALA456, VAL62, ILE221, MET210. The Pi-Pi stacked interactions were found with TYR214. The Pi-sulfur interactions with MET235. The Van der Waals interaction with TYR61, SER64, ARG250, GLU221.

As shown in Figure 7, the AM2 had Pi-Alkyl interactions with MET210, MET235, ILE211, VAL62, VAL452, LYS459, ILE159. The Pi-Pi stacked interactions were found with TYR214. Pi-Sigma interactions were found with ALA456 and VAL455. The Van der Waals interaction with GLU221, CYS220, THR65, TYR215, GLN98, ARG63 TYR61.

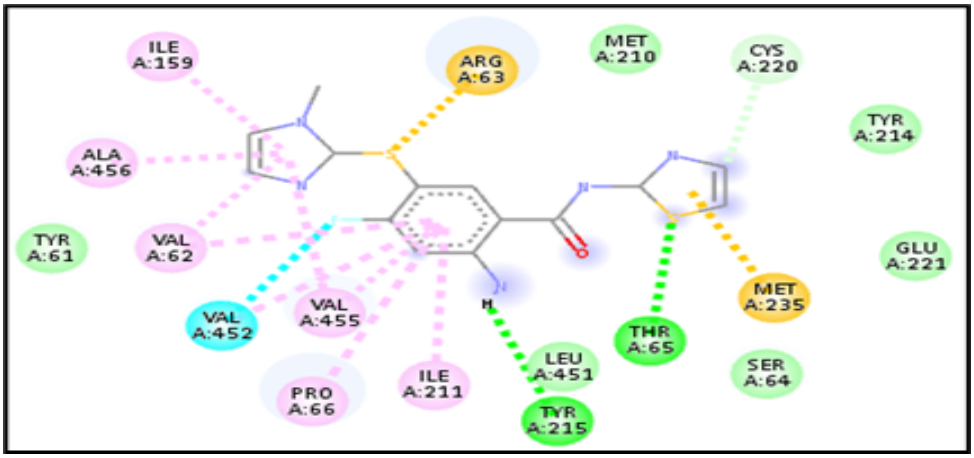

Figure 5. The **MRK** showing interactions in the GK.

As shown in Figure 8, the AM12 had hydrogen bond interactions with TYR215. The Pi-Alkyl interactions were found with ILE159, ALA456, VAL62, ILE221, MET210. The Pi-Pi stacked interactions were found with TYR214. The Van der Waals interaction with TYR61, SER64, ARG250, GLU221.

As shown in Figure 9, the AM17 had hydrogen bond interactions with THR65. The Pi-Alkyl interactions were found with ILE159, PRO66, VAL452, VAL62, ILE211, MET235. The Pi-Sigma interactions were found with ALA456, VAL455. The Van der Waals interaction with LYS459, TYR215, CYS220, TYR214, GLU221, ARG250, MET210, SER64, ARG63.

As shown in Figure 10, the AM58 had hydrogen bond interactions with THR65. The Pi-Alkyl interactions were found with MET235, ILE211, VAL62, ALA456, PRO66. The Pi-Sigma interactions were found with VAL455. The Van der Waals interaction with ARG250, GLU221, HIS218, ILE159, ARG63, MET210.

As shown in Figure 11, the AM5 had Pi-Alkyl interactions with ILE211, VAL452, PRO66, VAL62, ALA456, ILE159, LYS459. The Pi-Sigma interactions were found with VAL455. Pi-Sulfur interactions was found with MET235. The Pi-Pi T-shaped interaction was found with TYR214. The Van der Waals interaction with ARG250, GLU221, HIS218, ILE159, ARG63, MET210.

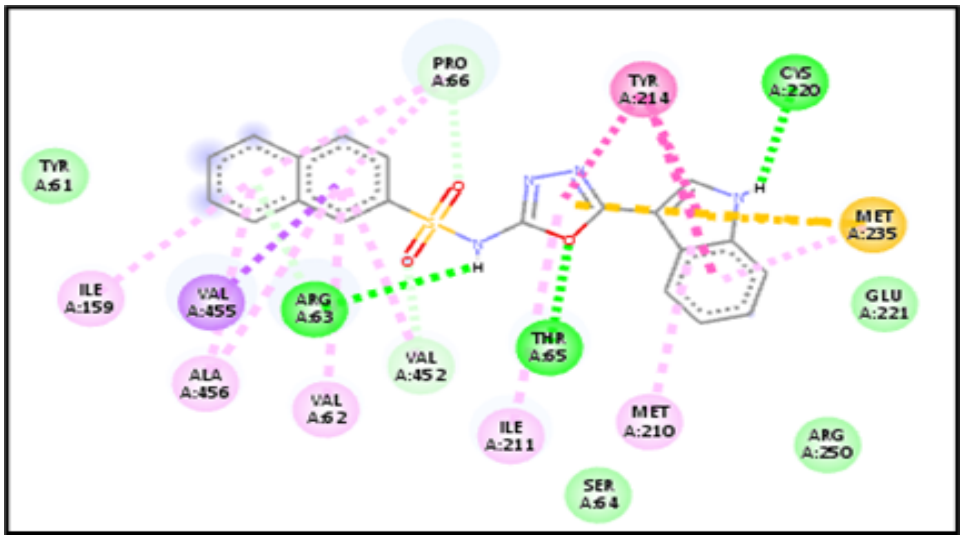

Figure 6. The AM35 showing interactions with GK.

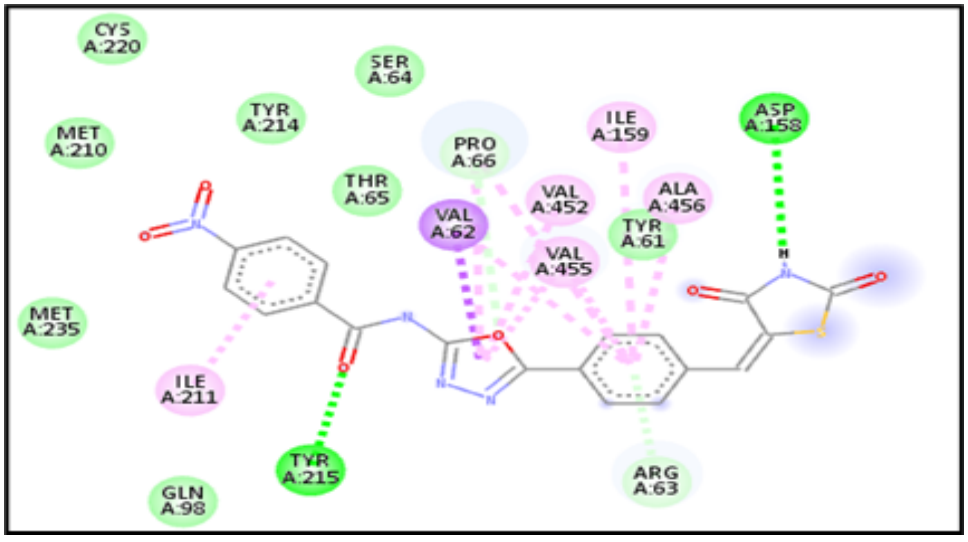

Figure 7. The AM2 showing interactions with GK.

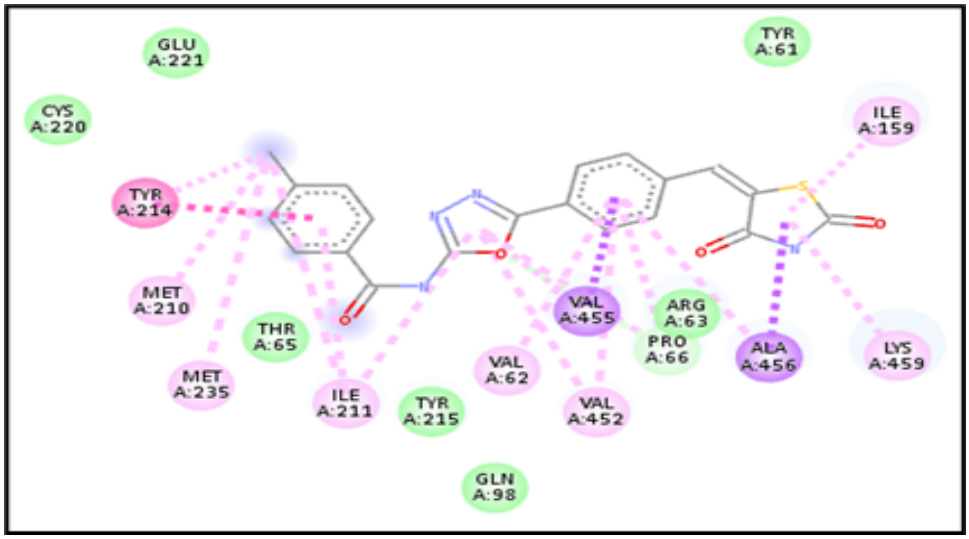

Figure 8. The AM12 showing interactions with GK.

As shown in Figure 12, the AM14 had Pi-Alkyl interactions with VAL452, VAL455, VAL62, ILE159, ARG63, LYS459. The Pi-Sigma interactions were found with VAL455. Pi-Sulfur interactions was found with MET235. The Pi-Pi T-shaped interaction was found with TYR214. The Van der Waals interaction with SER64, TYR215, ILE211, GLN98, TYR61, ASP158, THR65, PRO66, ALA456, ASP158.

As shown in Figure 13, the AM16 had Pi-Alkyl interactions with LYS459, ILE159, VAL62, VAL455, VAL452, ILE211, MET235. The Pi-Pi stacked interaction was found with TYR214. The Van der Waals interaction with ASP158, TYR61, TYR215, THR65, GLU221, MET210, CYS220, ALA456, PRO66.

As shown in Figure 16, the AM57 had hydrogen bond interactions with THR65. Pi-Alkyl interactions with PRO66, ALA456, VAL62, MET235. The Pi-Pi T shaped interactions were found with TYR214. Pi-cation interaction was found with ARG250. Pi-Sigma interaction was found with VAL455. The Van der Waals interaction with CYS220, TYR215, LEU451, ILE159, TYR61, SER64, MET210, ARG63.

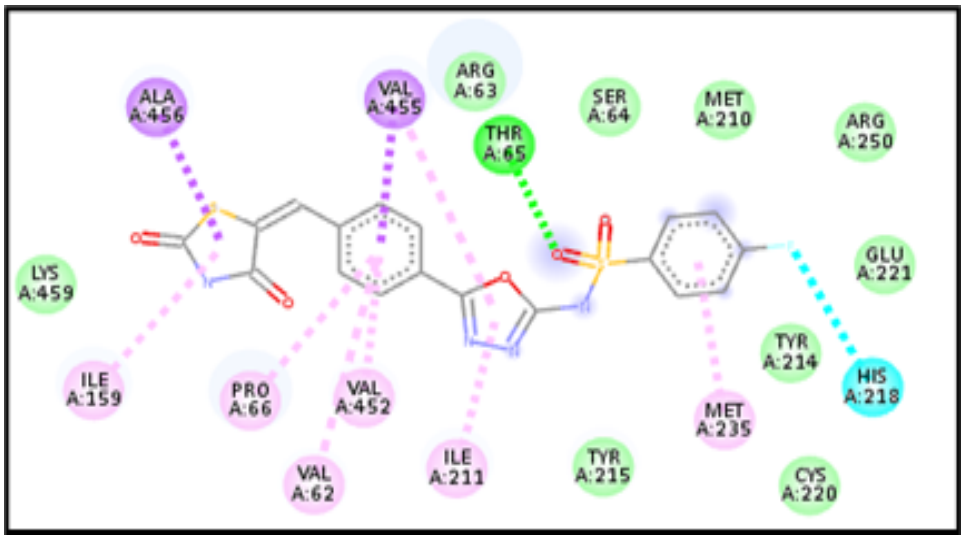

Figure 9. The AM17 showing interactions with GK

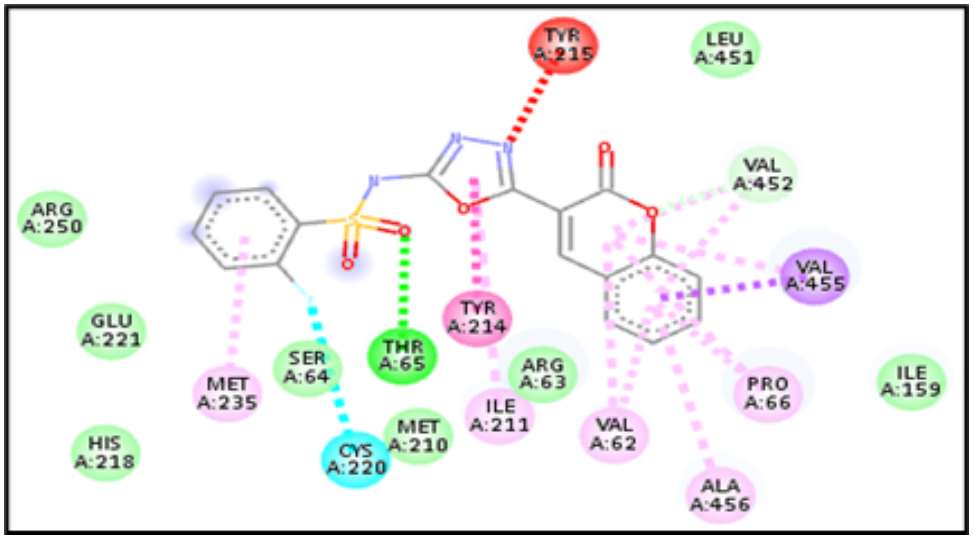

Figure 10. The AM58 showing interactions with GK

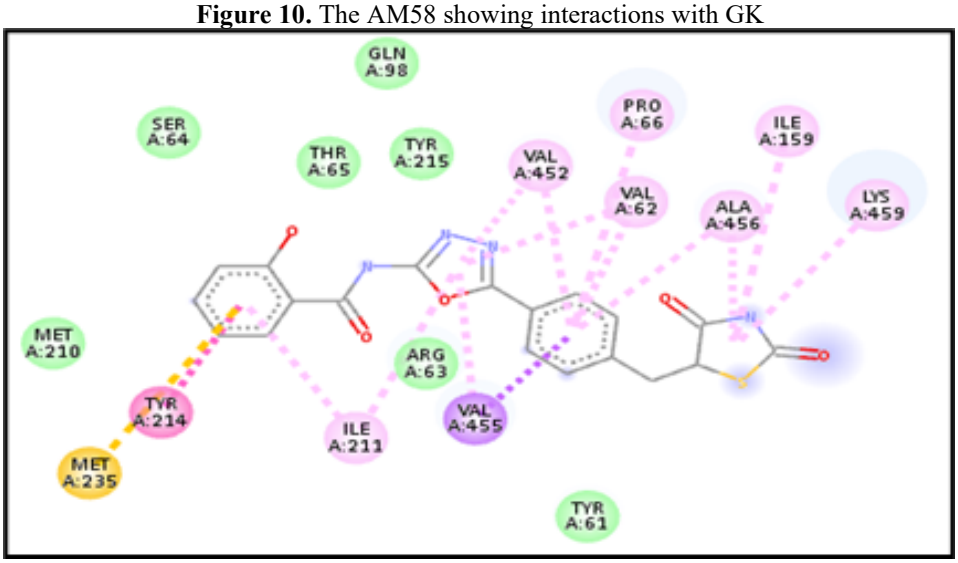

Figure 11. The AM5 showing interactions with GK.

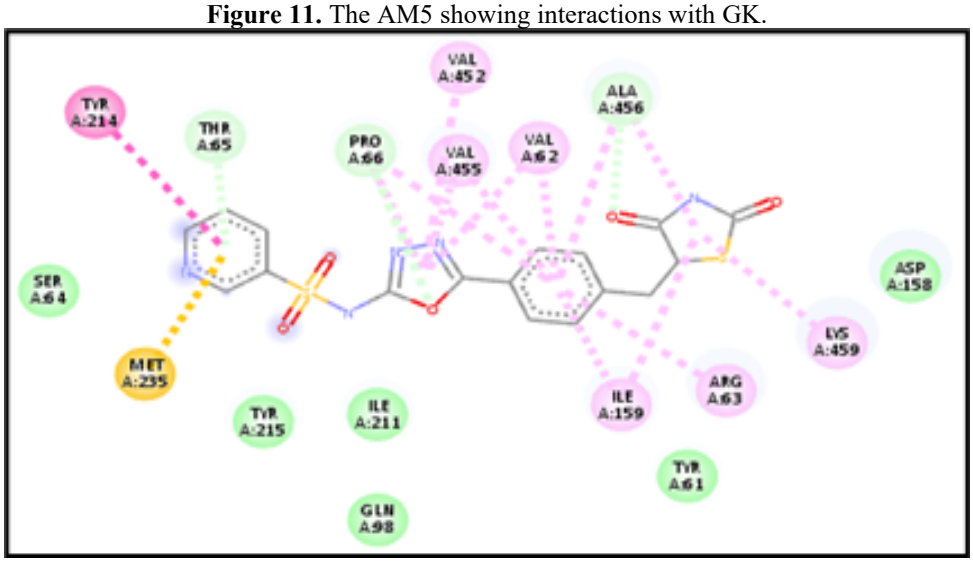

Figure 12. The AM14 showing interactions with GK.

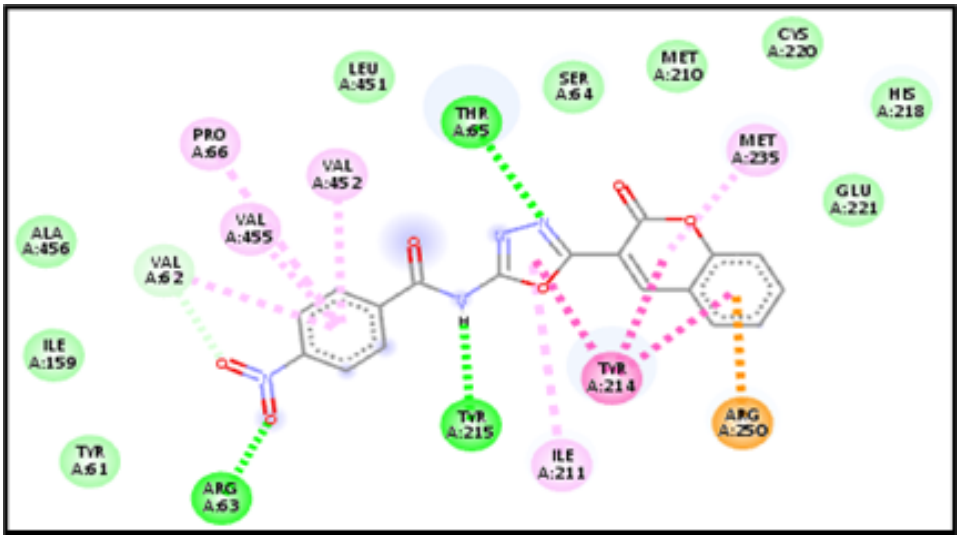

Figure 13. The **AM16** showing interactions with GK.

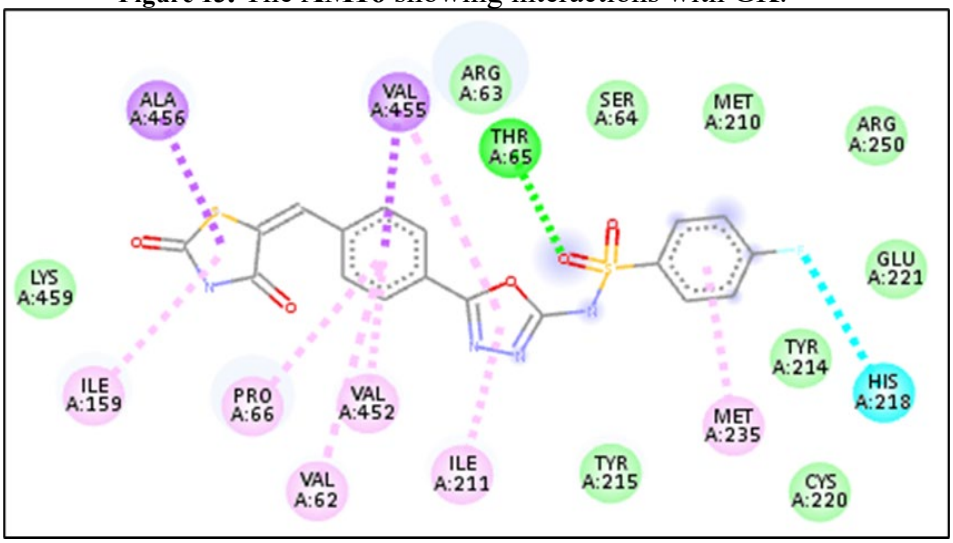

Figure 14. The AM19 showing interactions with GK.

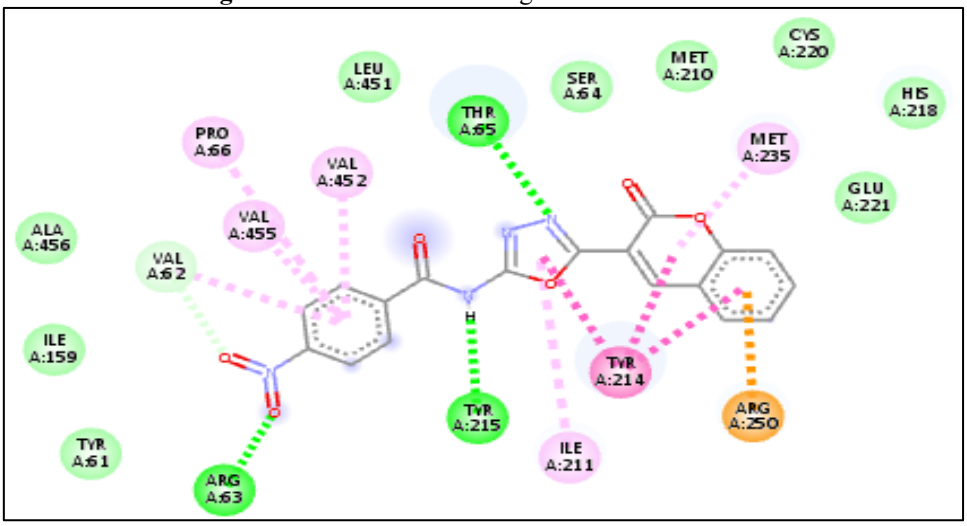

Figure 15. The **AM52** showing interactions with GK.

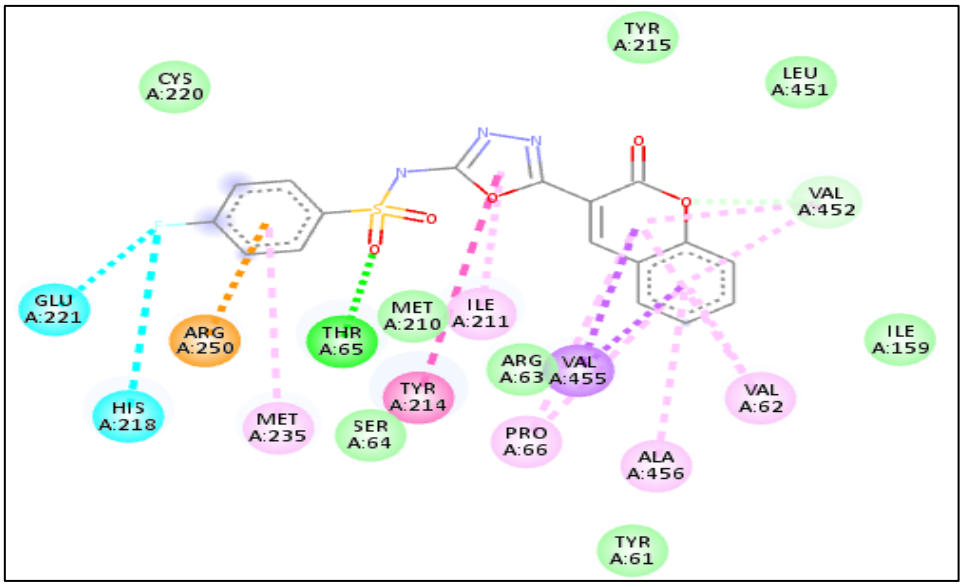

Figure 16. The **AM57** showing interactions with GK.

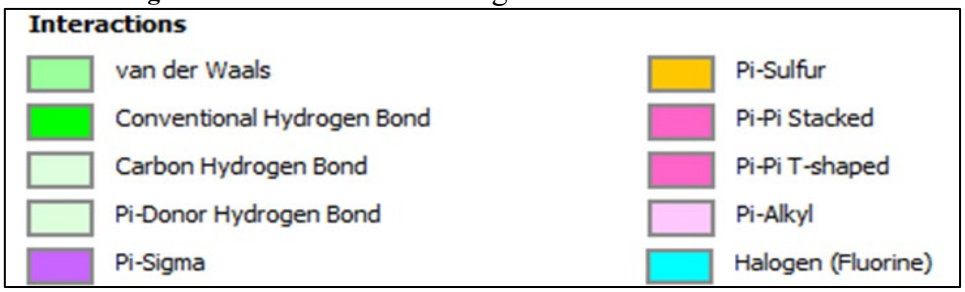

Table 2: The binding affinity of hit compounds with their hydrogen bond interactions and other interactions with neighbouring protein residues in GK active pockets.

Sr. No.	Compound	Binding affinity	H-bond	Pi-Alkyl	Pi-sigma	Pi-pi T-shaped
1	AM35	-11.6	ARG63 CYS220 THR65	ILE159 ALA456 VAL62 ILE221 MET210	-	TYR214
2	AM2	-11.3	TYR215	MET210 MET235 ILE211 VAL62 VAL452 LYS459 ILE159	ALA456 VAL455	TYR214
3	AM12	-11.1	THR65	ILE159 ALA456 VAL62 ILE221 MET210	-	-
4	AM17	-11.1	THR65	ILE159 PRO66 VAL452 VAL62 ILE211 MET235	ALA456 VAL455	-
5	AM58	-11.0	-	MET235 ILE211 VAL62 ALA456 PRO66	VAL455	TYR214
6	AM5	-11.0	-	ILE211 VAL452 PRO66 VAL62 ALA456 ILE159 LYS459	VAL455	TYR214
7	AM14	-10.8	-	VAL452 VAL455 VAL62 ILE159 ARG63 LYS459	VAL455	TYR214
8	AM16	-10.8	-	LYS459 ILE159 VAL62 VAL455 VAL452 ILE211 MET235	-	TYR214
9	AM19	-10.8	THR65	ILE159 PRO66 VAL62 VAL452 ILE211 MET235	VAL455 ALA456	-

10	AM52	-10.8	ARG63 TYR215 THR65	PRO66 VAL455 VAL452 ILE211 MET235	-	TYR214
11	AM57	-10.8	THR65	PRO66 ALA456 VAL62 MET235	VAL455	TYR214
12	MRK	-7.2	TYR215 THR65	ILE211 PRO66 VAL455 VAL62 ALA456 ILE159	-	-

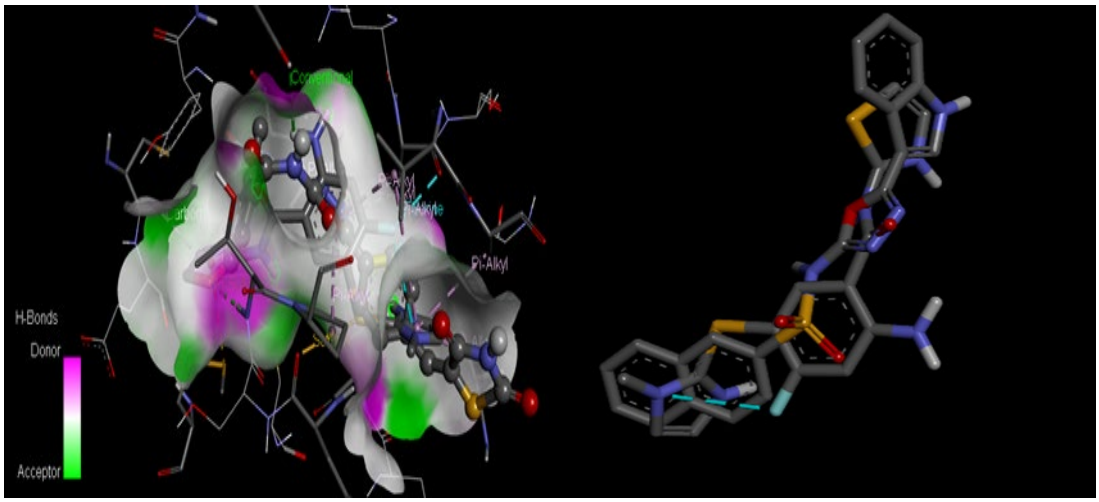

A **B**

Figure 17. A. Overlapping of co-crystallized ligand and designed ligands to ensure validation. **B**. Validation Pose of co-crystallized ligand and designed heterocyclic derivatives.

3.3. Molecular docking validation studies

Molecular docking protocols and methods (57) were validated by redocking the cocrystallized ligands at their crystal positions (Figure 17B) without introducing any conformers or changing their states. It was found that MRK's, RMSD values = 1 when the crystallographic conformation was superimposed on the cocrystallized ligand's docked position. Docking of molecular molecules is often done using RMSD (root mean square deviation) values to test the quality of the reproduction binding pose. In general, the bound structure prediction is considered to be accurate when the pose's RMSD is less than 1, while other values between 1 to 3, are deemed acceptable (58). Reproducibility had ensured for virtual screening results. In order to confirm consistency of the results, the virtual screening was reran using the same dataset and parameters. Additionally, among all poses, the one depicting ligand overlap with the cocrystallized ligand (Figure 17A) was chosen for evaluation regarding docking scores and interactions with amino acids.

3.4. ADME Analysis

A candidate molecule's physio-chemical properties had a significant impact on its fate. In table 3 the physiochemical characteristics of 11 hit compounds, such as their molecular weight, Log P value and hydrogen bond acceptors and donors. Bioavailability scores for the hit compounds were similar to the standard MRK, with a bioavailability score of 0.55. Using Lipinski's rule of five to evaluate the similarity of compounds to drugs, every hit compound passed the test. Among the eight compounds tested, compounds AM35 and AM2 showed the highest binding affinity, which was -11.6 and -11.3 Kcal/mol, respectively. AM35 and AM2 contains five hydrogen bond acceptors and 6 hydrogen bond acceptors respectively. Both these compounds showed 2 hydrogen bond donors. AM35 showed high GI absorption and were not able to cross the blood-brain barrier with Log P values of 2.41.

3.5. TOXICITY

Based on the provided data, the properties of compounds AM35, AM2, and the standard

compound MRK were analyzed, considering their AMES toxicity, MTD (human) log mg/kg/day, ORAT (LD50) mol/kg, hepatotoxicity, skin sensitization, T.Pyriformis toxicity log µg/mL, and minnow toxicity (mM). In terms of AMES toxicity, both AM2 and MRK are classified as non-AMES toxic, while AM35 falls into the category of AMES toxic. Concerning the MTD (human) log mg/kg/day, AM2 is associated with a positive value of 0.163, indicating a potential safe dosage, whereas AM35 exhibits a negative value (0.798), suggesting caution in determining the maximum tolerated dose.

Table 3. The drug-likeness property of hit heterocyclic derivatives using SwissADME tool.

Sr.no	Compound	MW	H-bond acceptor	H-bond donor	LOG P	GI absorption	BBB permeant	Bioavailability
1	AM35	390.42	5	2	2.41	High	No	0.55
2	AM2	426.83	6	2	2.44	Low	No	0.55
3	AM13	471.28	6	2	2.75	Low	No	0.55
4	AM12	437.39	8	2	1.86	Low	No	0.55
5	AM17	446.43	8	2	2.35	Low	No	0.55
6	AM58	387.34	8	1	2.45	High	No	0.55
7	AM5	408.39	7	3	1.91	Low	No	0.55
8	AM14	429.43	8	2	1.84	Low	No	0.55
9	AM16	458.47	8	2	2.44	Low	No	0.55
10	AM19	428.44	7	2	2.27	Low	No	0.55
11	AM52	378.30	8	1	1.97	Low	No	0.55
12	AM57	387.34	8	1	2.4	High	No	0.55
13	Co-cryst Ligand (MRK)	349.41	4	2	2	Low	No	0.55
14	Canagliflozin	444.52	6	4	3.27	High	No	0.55
15	Dapagliflozin	408.87	6	4	3.12	High	No	0.55
16	Dorzagliatin	462.93	6	3	3.08	High	No	0.55

MRK, Canagliflozin, Dapagliflozin, and Dorzagliatin fall within the range of 0.197-0.545 in this regard. Regarding ORAT (LD50) mol/kg, AM2 displays a higher value of 2.692, implying relatively lower toxicity when compared to AM35 (3.325) and MRK (0.969). All compounds show evidence of hepatotoxicity. In terms of skin sensitization, none of the compounds, including AM2, AM35, and MRK, exhibit signs of skin sensitization. For T.Pyriformis toxicity, AM2 registers a log µg/mL value of 0.338, whereas AM35 (0.285) has a slightly lower value of 0.319. MRK displays an equivalent value to that of AM35, at 0.285. Regarding minnow toxicity, AM35 demonstrates a lower toxicity level with a value of -0.233, while AM2 and MRK have values of -0.622 and 1.657, respectively, as shown in table 4. In summary, when comparing AM35, AM2, and MRK, AM2 exhibits favorable characteristics in terms of AMES toxicity, MTD (human) log mg/kg/day, ORAT (LD50) mol/kg, hepatotoxicity, T.Pyriformis toxicity, and minnow toxicity. However, a more comprehensive assessment and analysis are necessary to thoroughly evaluate these compounds and determine their suitability for specific applications.

Using a rational drug design approach, 60 heterocyclic derivatives were designed with the aim of evaluating their potential as antidiabetic agents, specifically targeting glucokinase (GKA). These molecules were subjected to molecular docking simulations to assess their binding to the glucokinase binding site. MRK (a co-crystallized ligand), Dorzagliatin (approved by the Japan FDA as a GKA), Dapagliflozin, and Canagliflozin were utilized as standard references and sought compounds not yet available on the market. The 2D and 3D structures of these designed compounds were generated using Chemdraw 2D and Chemdraw 3D, respectively, and their steric hindrances were minimized using MM2. Subsequently, the ligand was extracted from the glucokinase receptor protein, which was obtained from the Protein Data Bank. Autodock software was employed to investigate the binding affinities of all the compounds. Lead compounds with

binding affinities surpassing that of the conventional MRK molecule were identified, with Compound AM35 exhibiting the highest binding affinity at -11.6 Kcal/mol for the active GK site. Following the determination of binding affinities, the interactions between the protein and the molecules were visualized using PyMOL software, and further insights into these interactions were obtained using Discovery Studio. Key amino acid residues involved in interactions at the GK site were TYR214T, ILE159, ALA456, VAL62, ILE211, and MET210. Subsequently, 11 promising hit compounds were selected based on their binding affinities and subjected to pharmacokinetic profile prediction using SwissADME.

Table 4: Toxicity Profile of Potent compounds

Sr. no	Compound	AMES toxicity	MTD (human) log mg/kg/day	ORAT (LD50) mol/kg	Hepatotoxicity	Skin Sensitization	*T.Pyriformis* toxicity log µg/mL	Minnow toxicity (mM)
1	AM35	Yes	0.798	3.325	Yes	No	0.285	-0.233
2	AM2	No	0.163	2.692	Yes	No	0.338	-0.622
3	Co-cryst Ligand (MRK)	Yes	0.545	0.969	Yes	No	0.285	1.657
4	Canagliflozin	No	0.229	2.755	No	No	0.285	-0.499
5	Dapagliflozin	No	0.197	2.597	No	No	0.289	1.567
6	Dorzagliatin	No	0.428	3.328	Yes	No	0.308	2.394

*MTD = Max Tolerated Dose, ORAT = Oral Rat Acute Toxicity, LD50 = Lethal Dose

Among these hits, SwissADME indicated that compounds AM35 and AM2 possessed favorable pharmacokinetic profiles, including an optimal LogP value. Notably, all compounds met Lipinski's rule of five criteria, featuring a molecular weight below 500, fewer than 10 H-bond acceptors, fewer than 5 H-bond donors, and a LogP value below 5. Furthermore, these compounds exhibited high gastrointestinal (GI) absorption, enhancing their potential for systemic absorption and therapeutic efficacy. This characteristic is pivotal for drug candidates. In conclusion, the analysis of SwissADME profiles, adherence to Lipinski's rule of five, high GI absorption, and no potential blood-brain barrier (BBB) permeability collectively suggest that these compounds possess promising drug-like properties. Extensive investigations and evaluations are warranted to explore their therapeutic applications, particularly in the context of type 2 diabetes. Experimental studies using organism models like Streptozotocin induced diabetic rat model may also provide insights into their potential as lead molecules with potent glucokinase activity for treating type 2 diabetes.

As well as contributing to the advancement of computational methodologies in drug development, these novel heterocyclic derivatives provide insights into their efficacy as Glucokinase activators. Providing improved Glucokinase activation compared to existing standards, the results of this study might provide a new class of compounds. This has profound implications for conditions related to glucose metabolism, potentially opening avenues for more effective therapeutic interventions.

4. Conclusions

In summary, our study encompassed a thorough rational design of 60 novel heterocyclic derivatives, with the primary objective of identifying potential lead compounds with potent glucokinase (GK) activation capabilities for treating type 2 diabetes. These compounds underwent docking studies against the GK binding site, and their 2D and 3D structures were scrutinized through Chemdraw software. MM2 was used to minimize steric hindrance in their structures and Autodock software to assess their binding affinities. Based on these binding affinities, Compound AM35 emerged as the most promising candidate, boasting the highest binding affinity of -11.6 Kcal/mol for the active GK site. Further analysis of the interaction between these compounds and the protein was conducted using Pymol and Discovery Studio, revealing significant interactions with amino acid residues TYR214T, ILE159, ALA456, VAL62, ILE211, and MET210 within the GK site. Then the selected compounds were subjected to pharmacokinetic profile prediction using SwissADME. Among these compounds, AM35 and AM2 exhibited favorable

pharmacokinetic profiles with optimal LogP values. Notably, all analyzed compounds had a molecular weight below 500, aligning with the criteria for assessing drug-like properties and adhering to Lipinski's rule of five. Additionally, our designed compounds demonstrated high gastrointestinal absorption, signifying their potential for efficient bloodstream absorption—an essential attribute for drug candidates. In summary, our findings underscore the promising drug-like properties of these compounds, with AM2 standing out as a potential lead molecule for further development. Comparing the compounds AM35, AM2, and MRK based on various toxicity and safety parameters provides valuable insights. AM2 presents a favorable profile with non-AMES toxicity, a positive MTD (human) log mg/kg/day value indicating potential safe dosage, a higher ORAT (LD50) mol/kg value indicating lower toxicity, non-hepatotoxicity, no skin sensitization, moderate T.Pyriformis toxicity, and lower minnow toxicity. In contrast, AM35 exhibits AMES toxicity, a negative MTD (human) log mg/kg/day value warranting caution in determining the maximum tolerated dose, a relatively lower ORAT (LD50) mol/kg value indicating higher toxicity, non-hepatotoxicity, no skin sensitization, lower T.Pyriformis toxicity, and moderate minnow toxicity. MRK, being the standard compound, shows AMES toxicity, a negative MTD (human) log mg/kg/day value, a moderate ORAT (LD50) mol/kg value, hepatotoxicity, no skin sensitization, higher T.Pyriformis toxicity, and moderate minnow toxicity. Taking these findings into account, AM35 presents a more promising toxicity and safety profile compared to AM2 and MRK. Nonetheless, it is vital to emphasize that comprehensive studies and evaluations are imperative to fully grasp the potential risks and benefits associated with these compounds and their suitability for specific applications. Future investigations should prioritize conducting experimental studies using organism models such as the Streptozotocin-induced diabetic rat model to assess the compounds' glucokinase activation potential and explore their therapeutic applications in treating type 2 diabetes.

ACKNOWLEDGEMENT

The authors would like to acknowledge Lovely Professional University, Jalandhar, India for their continuous support and encouragement.

References

[1] Ahmad E, Lim S, Lamptey R, Webb DR, Davies MJ. Type 2 diabetes, The Lancet, 400 (2022) 1803-1820.

[2] Ashcroft FM, Lloyd M, Haythorne EA. Glucokinase activity in diabetes: too much of a good thing?, Trends in Endocrinology & Metabolism, 34 (2023) 119-130.

[3] Artasensi A, Pedretti A, Vistoli G, Fumagalli L. Type 2 diabetes mellitus: a review of multi-target drugs, Molecules, 25 (2020) 1987.

[4] Diaz-Santana MV, O'Brien KM, Park YM, Sandler DP, Weinberg CR. Persistence of risk for type 2 diabetes after gestational diabetes mellitus, Diabetes Care, 45 (2022) 864-870.

[5] Akhtar S, Nasir JA, Ali A, Asghar M, Majeed R, Sarwar A. Prevalence of type-2 diabetes and prediabetes in Malaysia: A systematic review and meta-analysis, PloS one, 17 (2022) e0263139.

[6] Saleh M, Kim JY, March C, Gebara N, Arslanian S. Youth prediabetes and type 2 diabetes: risk factors and prevalence of dysglycaemia, Pediatric Obesity, 17 (2022), e12841.

[7] Thilagavathi R, Hosseini-Zare MS, Malini M, Selvam C. A comprehensive review on glucokinase activators: Promising agents for the treatment of Type 2 diabetes, Chemical Biology & Drug Design, 99 (2022) 247-263.

[8] Sharma S, Wadhwa K, Choudhary M, Budhwar V. Ethnopharmacological perspectives of glucokinase activators in the treatment of diabetes mellitus, Natural Product Research, 36 (2022) 2962-2976.

[9] Kroon T, Hagstedt T, Alexandersson I, Ferm A, Petersson M, Maurer S, Zarrouki B, Wallenius K, Oakes ND, Boucher J. Chronotherapy with a glucokinase activator profoundly improves metabolism in obese Zucker rats, Science Translational Medicine, 14 (2022) eabh1316.

[10] Khan A, Unnisa A, Sohel M, Date M, Panpaliya N, Saboo SG, Siddiqui F, Khan S. Investigation of phytoconstituents of Enicostemma littorale as potential glucokinase activators through molecular docking for the treatment of type 2 diabetes mellitus, In Silico Pharmacology, 10 (2022) 1-6.

[11] Sharma P, Singh S, Sharma N, Singla D, Guarve K, Grewal AS. Targeting human Glucokinase for the treatment of type 2 diabetes: an overview of allosteric Glucokinase activators, Journal of Diabetes & Metabolic Disorders, 21 (2022) 1129-1137.

[12] Kawata S, Nakamura A, Miyoshi H, Yang K, Shigesawa I, Yamauchi Y, Tsuchida K, Omori K, Takahashi K, Nomoto H, Kameda H. Glucokinase activation leads to an unsustained hypoglycaemic effect with hepatic triglyceride accumulation in db/db mice. Diabetes, Obesity and Metabolism, 24 (2022) 391-401.

[13] Yang W, Wu H, Cai X, Lin C, Jiao R, Ji L. Evaluation of efficacy and safety of glucokinase activators—a systematic review and meta-analysis, Frontiers in Endocrinology, 14 (2023) 1175198.

[14] Miao J, Fu P, Ren S, Hu C, Wang Y, Jiao C, Li P, Zhao Y, Tang C, Qian Y, Yang R. Effect of renal impairment on the pharmacokinetics and safety of dorzagliatin, a novel dual-acting glucokinase activator, Clinical and Translational Science, 15 (2022) 548-557.

[15] Tsumura Y, Tsushima Y, Tamura A, Kato H, Kobayashi T. Disruptions in hepatic glucose metabolism are involved in the diminished efficacy after chronic treatment with glucokinase activator, Plos one, 17 (2022) e0265761.

[16] Bahl V, May CL, Perez A, Glaser B, Kaestner KH. Genetic activation of α-cell glucokinase in mice causes enhanced glucose-suppression of glucagon secretion during normal and diabetic states, Molecular Metabolism, 49 (2021) 101193.

[17] Liu D, Du Y, Yao X, Wei Y, Zhu J, Cui C, Zhou H, Xu M, Li H, Ji L. Safety, tolerability, pharmacokinetics, and pharmacodynamics of the glucokinase activator PB-201 and its effects on the glucose excursion profile in drug-naïve Chinese patients with type 2 diabetes: a randomised controlled, crossover, single-centre phase 1 trial, EClinicalMedicine, 42 (2021) 101185.

[18] Li C, Zhang Y, Chen L, Li X. Glucokinase and glucokinase activator, Life Metabolism, 2 (2023) load031.

[19] Cai N, Chen X, Liu J, Wen Z, Wen S, Zeng W, Lin S, Chen Y, Shi G, Zeng L. Glucokinase activator improves glucose tolerance and induces hepatic lipid accumulation in mice with diet-induced obesity, Liver Research, 7 (2023) 124-135.

[20] Malini M, Thilagavathi R, Kumar Singh S, Pravin A, Selvam C. Structure-Based Drug Design: Identification of Glucokinase Activators from Natural Compounds for the Treatment of Type 2 Diabetes, ChemistrySelect, 8 (2023) e202204909.

[21] Remedi MS, Nichols CG. Glucokinase Inhibition: A Novel Treatment for Diabetes?, Diabetes, 72 (2023) 170-174.

[22] Ren Y, Li L, Wan L, Huang Y, Cao S. Glucokinase as an emerging anti-diabetes target and recent progress in the development of its agonists, Journal of Enzyme Inhibition and Medicinal Chemistry, 2022 37(2023) 606-615.

[23] Chavan A, Daniel K, Patel AM. In-silico Exploration of Phytoconstituents of Gymnema sylvestre as Potential Glucokinase Activators and DPP-IV Inhibitors for the Future Synthesis of Silver Nanoparticles for the Treatment of Type 2 Diabetes Mellitus, Current Enzyme Inhibition, 18 (2022) 47-60.

[24] Kazi AA, Chatpalliwar VA. Design, Synthesis, Molecular Docking and In vitro Biological Evaluation of Benzamide Derivatives as Novel Glucokinase Activators, Current Enzyme Inhibition, 18 (2022) 61-75.

[25] Yadav S, Bharti S, Mathur P. GlucoKinaseDB: A comprehensive, curated resource of glucokinase modulators for clinical and molecular research, Computational Biology and Chemistry, 103 (2023) 107818.

[26] Santos-Ballardo CL, Montes-Ávila J, Rendon-Maldonado JG, Ramos-Payan R, Montaño S, Sarmiento-Sánchez JI, de Jesús Acosta-Cota S, Ochoa-Terán A, de Jesús Bastidas-Bastidas P, Osuna-Martínez U. Design, synthesis, in silico, and in vitro evaluation of benzylbenzimidazolone derivatives as potential drugs on α-glucosidase and glucokinase as pharmacological targets, RSC Advances, 13 (2023) 21153-21162.

[27] Sharma P, Thakur A, Goyal A, Grewal AS. Molecular docking, 2D-QSAR and ADMET studies of 4-sulfonyl-2-pyridone heterocycle as a potential glucokinase activator, Results in Chemistry, 6 (2023) 101105.

[28] Hamid AA, Abdul-Rasheed OF, Mahdi MF, Atia AJ. Design, synthesis, characterization, and biological evaluation of new diazole-

benzamide derivatives as glucokinase activators with antihyperglycemic activity, Egyptian Journal of Chemistry, 65 (2022) 451-469.

[29] Kazi AA, Chatpalliwar VA. Design, Synthesis, Molecular Docking and In vitro Biological Evaluation of Benzamide Derivatives as Novel Glucokinase Activators, Current Enzyme Inhibition, 18 (2022) 61-75.

[30] Arora S, Grewal AS, Sharma N, Arora K, Dhalio E, Singh S. Design, synthesis, and evaluation of some novel N-benzothiazol-2-yl benzamide derivatives as allosteric activators of human glucokinase, Journal of Applied Pharmaceutical Science, 11 (2021) 38-47.

[31] Khadse SC, Amnerkar ND, Dighole KS, Dhote AM, Patil VR, Lokwani DK, Ugale VG, Charbe NB, Chatpalliwar VA. Hetero-substituted sulfonamido-benzamide hybrids as glucokinase activators: Design, synthesis, molecular docking and in-silico ADME evaluation, Journal of Molecular Structure, 1222 (2020) 128916.

[32] Khadse SC, Amnerkar ND, Dave MU, Lokwani DK, Patil RR, Ugale VG, Charbe NB, Chatpalliwar VA. Quinazolin-4-one derivatives lacking toxicity-producing attributes as glucokinase activators: design, synthesis, molecular docking, and in-silico ADMET prediction, Future Journal of Pharmaceutical Sciences, 5 (2019) 1-4.

[33] Grewal AS, Kharb R, Prasad DN, Dua JS, Lather V. N-pyridin-2-yl benzamide analogues as allosteric activators of glucokinase: Design, synthesis, in vitro, in silico and in vivo evaluation, Chemical Biology & Drug Design, 93 (2019) 364-372.

[34] Charaya N, Pandita D, Grewal AS, Lather V. Design, synthesis and biological evaluation of novel thiazol-2-yl benzamide derivatives as glucokinase activators, Computational Biology and Chemistry, 73 (2018) 221-229.

[35] Kohn TJ, Du X, Lai S, Xiong Y, Komorowski R, Veniant M, Fu Z, Jiao X, Pattaropong V, Chow D, Cardozo M. 5-Alkyl-2-urea-substituted pyridines: identification of efficacious glucokinase activators with improved properties, ACS Medicinal Chemistry Letters, 7 (2016) 666-670.

[36] Kaur A, Thakur S, Deswal G, Chopra B, Dhingra AK, Guarve K, Grewal AS. In silico docking based screening of constituents from Persian shallot as modulators of human glucokinase, Journal of Diabetes & Metabolic Disorders, 22 (2023) 547-570.

[37] YANG W. 860-P: Evaluation of Efficacy and Safety of Glucokinase Activators-A Systematic Review and Meta-analysis, Diabetes, 72 (2023) 860.

[38] Ren Y, Li L, Wan L, Huang Y, Cao S. Glucokinase as an emerging anti-diabetes target and recent progress in the development of its agonists, Journal of Enzyme Inhibition & Medicinal Chemistry, 37 (2022) 606-615.

[39] Gao Q, Zhang W, Li T, Yang G, Zhu W, Chen N, Jin H. The efficacy and safety of glucokinase activators for the treatment of type-2 diabetes mellitus: a meta-analysis, Medicine, 100 (2021) 40.

[40] Liu J, Fu H, Kang F, Ning G, Ni Q, Wang W, Wang Q. β-Cell glucokinase expression was increased in type 2 diabetes subjects with better glycemic control. Journal of Diabetes. 15 (2023) 409-418.

[41] Paliwal A, Paliwal V, Jain S, Paliwal S, Sharma S. Current Insight on the Role of Glucokinase and Glucokinase Regulatory Protein in Diabetes, Mini Reviews in Medicinal Chemistry, 24 (2023) 674-688.

[42] Chakera AJ, Steele AM, Gloyn AL, Shepherd MH, Shields B, Ellard S, et al. Recognition and management of individuals with hyperglycemia because of a heterozygous glucokinase mutation, Diabetes Care, 38 (2015) 1383–1392.

[43] Song L, Cao F, Niu S, Xu M, Liang R, Ding K, Lin Z, Yao X, Liu D. Population Pharmacokinetic/Pharmacodynamic Analysis of the Glucokinase Activator PB201 in Healthy Volunteers and Patients with Type 2 Diabetes Mellitus: Facilitating the Clinical Development of PB201 in China, Clinical Pharmacokinetics, 63 (2024) 93-108.

[44] Kazi AA, Chatpalliwar VA. Design, Synthesis, Molecular Docking and In vitro Biological Evaluation of Benzamide Derivatives as Novel Glucokinase Activators, Current Enzyme Inhibition, 18 (2022) 61-75.

[45] Kamata K, Mitsuya M, Nishimura T, Eiki JI, Nagata Y. Structural basis for allosteric regulation of the monomeric allosteric enzyme human glucokinase, Structure, 12 (2004) 429-438.

[46] Taherkhani A, Orangi A, Moradkhani S, Khamverdi Z. Molecular docking analysis of flavonoid compounds with matrix metalloproteinase-8 for the identification of potential effective inhibitors, Letters in Drug Design & Discovery, 18 (2021) 16-45.

[47] Souza PF, Lopes FE, Amaral JL, Freitas CD, Oliveira JT. A molecular docking study revealed that synthetic peptides induced conformational changes in the structure of SARS-CoV-2 spike glycoprotein, disrupting the interaction with human ACE2 receptor, International Journal of Biological Macromolecules, 164 (2020) 66-76.

[48] Mhaske GS, Sen AK, Shah A, Khiste RH, Dale AV, Sen DB. In Silico Identification of Novel Quinoline-3-carboxamide Derivatives Targeting Platelet-Derived Growth Factor Receptor, Current Cancer Therapy Reviews, 18 (2022) 131-142.

[49] Tabassum H, Ahmad IZ. Molecular docking and dynamics simulation analysis of thymoquinone and thymol compounds from Nigella sativa L. that inhibit cag A and Vac A oncoprotein of helicobacter pylori: Probable treatment of H. pylori Infections, Medicinal Chemistry, 17 (2021) 146-157.

[50] Athalye M, Teli D, Sharma A, Patel M. Anti-Epileptic Drug-Lipid Conjugates for Delivery to the Brain: In Silico ADMET Prediction, Molecular Docking and Molecular Dynamics Simulations, ChemistrySelect, 8 (2023) e202301701.

[51] Institute of Materia Medica, Chinese Academy of Medical Sciences. Preparation of thiazolidinedione derivatives as dual agonists of glucokinase and peroxisome proliferator-activated receptors. CN102558167; 2012.

[52] Cadila Healthcare Limited, Zydus Tower, Gujarat. Disubstituted benzamide derivatives as glucokinase (gk) activators. WO2010150280; 2010.

[53] Cadila Healthcare Limited, Zydus Tower, Gujarat. Substituted benzamide derivatives as glucokinase (gk) activators. WO2011013141; 2011.

[54] Yasuma T, Ujikawa O. Glucokinase activator compounds, methods of activating glucokinase and methods of treating diabetes and obesity. US8957070B2, 2015.

[55] Lin S Dewnani S, Kats-kagan R, Zhang R. Glucokinase Activators. WO2014099578A1, 2014.

[56] Grewal AS, Arora S, Sharma N, Singh S. In silico docking studies of compounds from Persian shallot as allosteric glucokinase activators, Plant Arch, 20 (2020) 3768-3771.

[57] Şenol H, Ağgül AG, Atasoy S, Güzeldemirci NU. Synthesis, characterization, molecular docking and in vitro anti-cancer activity studies of new and highly selective 1, 2, 3-triazole substituted 4-hydroxybenzohyrdazide derivatives, Journal of Molecular Structure, 1283 (2023) 135247.

[58] Tokalı FS, Taslimi P, Sadeghi M, Şenol H. Synthesis and Evaluation of Quinazolin-4 (3H)-one Derivatives as Multitarget Metabolic Enzyme Inhibitors: A Biochemistry-Oriented Drug Design, ChemistrySelect, 8 (2023) e202301158.